Vietnam Journal of Science and Technology ***62*** *(5) (2024) 965-978*

doi:10.15625/2525-2518/19566

Research on adsorption of Ni^{2+} ions using halloysite clay and the ability of desorption and nickel recovery by electrochemical method

Le Thi Duyen[1, 3, 4, *], Le Thi Phuong Thao[1, 3, 4], Cong Tien Dung[1, 4], Nguyen Viet Hung[1, 3, 4], Ha Manh Hung[1, 4], Mai Van Tien[5], Nguyen Thi Thanh Thao[2, 3], Bui Hoang Bac[2, 3]

[1]*Department of Chemistry, Faculty of Basic Science, Hanoi University of Mining and Geology, 18 Vien Street, Duc Thang, Bac Tu Liem, Ha Noi, Viet Nam*

[2]*Faculty of Geosciences and Geology Engineering, Hanoi University of Mining and Geology, 18 Vien Street, Duc Thang, Bac Tu Liem, Ha Noi, Viet Nam*

[3]*HiTech-CEAE Research Team, Hanoi University of Mining and Geology, 18 Vien Street, Duc Thang, Bac Tu Liem, Ha Noi, Viet Nam*

[4]*BSASD Research Group, Hanoi University of Mining and Geology, 18 Vien Street, Duc Thang, Bac Tu Liem, Ha Noi, Viet Nam*

[5]*Department of Environment, Hanoi University of Natural Resources and Environment, 41A Phu Dien Street, Bac Tu Liem District, Ha Noi, Viet Nam*

[*]Email: *lethiduyen@humg.edu.vn*

Received: 4 December 2023; Accepted for publication: 1 May 2024

Abstract. In this work, we studied the ability of adsorption of Ni^{2+} ions from aqueous solution using halloysite clay (HAL), which was taken from Thach Khoan area, Phu Tho province, Viet Nam, then desorption of Ni^{2+} from HAL and recovery of Ni metal. The light-yellow HAL powder had a specific surface area of 20.152 m^2/g with particle sizes smaller than 32 µm. The adsorption efficiency and capacity obtained under suitable conditions (0.8 g of HAL per 50 mL of solution, Ni^{2+} initial concentration of 50 mg/L, contact time of 80 minutes, pH_0 of 5.9, and at room temperature of 30 ^oC) were 82.59 % and 2.58 mg/g, respectively. The results of adsorption stoichiometry of Ni^{2+} ions on the HAL adsorbent were fitted to the Langmuir adsorption isotherm model (R^2 = 0.9931) with a maximum monolayer adsorption capacity of 3.739 mg/g. The adsorption process obeyed a pseudo-second-order kinetic model with R^2 = 0.9911. The process of desorption of Ni^{2+}ions from loaded HAL material and recovery of Ni metal was conducted in a deep eutectic solvent (reline) using electrodeposition method. The results showed that 92.65 % of Ni metal could be recovered after 5 hours with an applied current of 7.5 mA at 60 °C**.**

Keywords: Halloysite, adsorption of Ni^{2+} ions, recovery of Ni, electrodeposition.

Classification numbers: 3.4.2

1. INTRODUCTION

In modern life, the advancement in industry and urbanization has led to serious metal pollution all over the world [1]. Heavy metal ions are not decomposed or transformed into

substances that are not dangerous to humans, but are accumulated and deposited in the environment, leading to exceeding permissible limits and causing environmental imbalance. Exposure to heavy metals in the environment eventually leads to an increase in the levels of heavy metal ions in animals and humans through the food chain and can cause diseases such as neurological disorders, anemia, cancer, etc. [2]. Among them nickel is a useful metal, and people's demand for nickel is increasing while nickel mines are increasingly exhausted. It is essential to recover nickel from waste sources to avoid environmental pollution and to utilize it. Nickel is a transition metal that is silvery-white, hard, ductile, highly corrosion-resistant, easy to make alloy and could provide the alloy with high thermal stability, strength, high corrosion resistance, good mechanical and electrochemical properties. Nickel alloy is applied in many fields, such as stainless steel, mineral processing, metal finishing, coinage, battery manufacturing, metal alloys, electroplating, power plant industries, hydrometallurgical industry, zinc base casting, leather tanning and bioelectrochemical systems [3, 4]. As a consequence, the concentrations of nickel in various environmental compartments have been found to remarkably exceed natural levels. This causes harmful and dangerous effects on humans and the environment as nickel compounds and metallic nickel are carcinogens if the allowable level is exceeded [5]. It is clear that the reduction of nickel in the environment is an essential issue and has been studied. Among the Ni treatment methods, adsorption is a widely used and is considered an effective method due to its cost-effectiveness, rapidness, easiness of application, effectiveness also for low pollutant concentrations, and production of non-toxic by-products [6]. Ni absorbent materials can be divided into 7 groups, including carbonaceous materials (such as activated carbon), industrial and agricultural wastes, polymeric adsorbents, minerals, bioadsorbents (algae, bacteria), composites, and adsorbents with a special structure (nanomaterials, mesoporous materials) [3].

Clays are finely grained natural rocks mainly composed of aluminosilicates. As clay is mostly negatively charged, they are particularly efficacious for adsorption of metal cations. Kaolinite, bentonite, illite, and montmorillonite are the main types of clays that possess suitable characteristics for metal adsorption [3]. In addition, large availability, low cost, non-toxicity, non-flammability, and high specific surface area are further advantages of such minerals.

Natural halloysite material (HAL) is a clay mineral belonging to the kaolin group, which is also applied in many fields: pharmaceutical, medicine, food, high-grade materials and environment due to its superior properties such as microstructuretube, non-toxicity, and high mechanical strength [7, 8]. Furthermore, HAL has shown wide target capability, not only handling heavy metal ions well but also dealing well with anions and organic pigments [9-12]. In this paper, a detailed study on the Ni adsorption capacity of HAL in Thach Khoan area, Phu Tho province, Viet Nam is presented. This natural HAL material has been used to adsorb Cd and Pb with a high adsorption efficiency of 51.45 and 79.3 %, respectively [13].

In addition to heavy metal adsorption studies, it is very important to research and find effective methods of desorption, recovery of heavy metals and regeneration of adsorbent materials, minimizing negative impacts on the environment. There have been some published studies on desorption and recovery of heavy metals from hydroxyapatite [14 - 20], vermiculite [21], and kaolinite [22 - 25]. Several publications have presented nickel deposition from deep eutectic solvent (DES) formed from choline chloride [26 - 29]. In this work, we studied the adsorption of Ni^{2+} ions on HAL clay, followed by desorption and recovery of Ni metal from adsorbed HAL material by electrolysis in reline electrolyte (choline chloride-urea) as a green electrolyte. The advantage of this study is that the desorption and nickel recovery are carried out together in one electrochemical cell, after which the HAL adsorbent can be reused.

2. EXPERIMENTAL

2.1. Preparation of HAL powder

The halloysite samples studied were taken after the selection process at kaolin mines in Lang Dong, Thach Khoan, Phu Tho province, Viet Nam. The samples were then thoroughly mixed and filtered using a 32 µm mesh wet sieve. The samples under the sieve were decanted and dried at 60 °C. After drying, the samples were used for experiments and analysis in the next steps. To check the existence of halloysite in the samples, the analytical methods of scanning electron microscopy (SEM) combined with energy dispersive X-ray spectroscopy (EDS) (Quanta 450 - FEI at the Hanoi University of Mining and Geology, Viet Nam) and transmission electron microscope (TEM) (TEM 1010 - Jeol machine at the Vietnam Academy of Science and Technology) were used. The phase composition of halloysite was determined by X-ray diffraction (XRD) method conducted on a Siemens D5005 machine at the University of Natural Science - Hanoi National University, Viet Nam (Bui Hoang Bac *et al.*, 2021). HAL powder was light yellow (Figure 1) and had a nanotube shape (Figure 2) with a specific surface area (BET) of 20.152 m^2/g.

Figure 1. Image of halloysite powder.

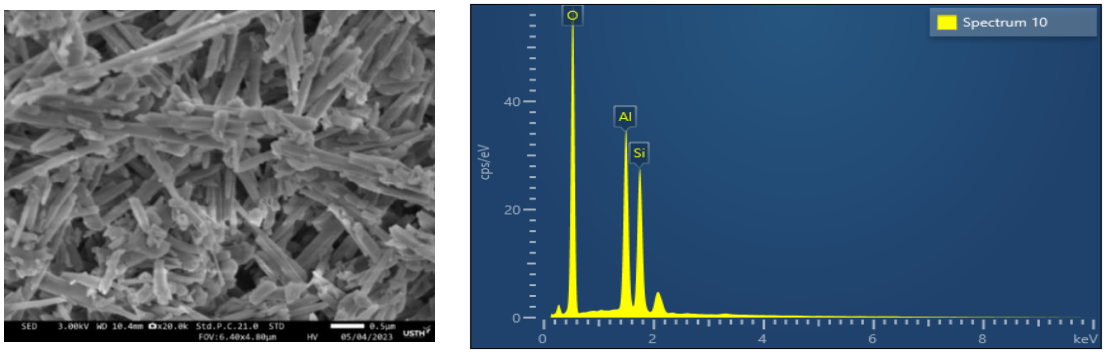

Figure 2. SEM-EDX image of halloysite.

2.2. Preparation of reline deep eutectic solvent (DES)

The reline DES was obtained by mixing choline chloride (ChCl) (Alfa Aesar, 98 %) and urea (U). Choline chloride was recrystallized from absolute ethanol, filtered and dried under vacuum. Choline chloride and urea were mixed in a molar ratio of 1:2 in a closed container under constant stirring for 3 hours at 60 ^oC until a homogeneous colorless liquid was formed.

2.3. Determination of pH_{PZC} of HAL powder

A mixture of 0.5 g of HAL powder in 50 mL of 0.01 M KNO_3 solution was stirred for 60 minutes at room temperature. The initial pH values (pH_0) were adjusted in the range of 2.5 - 9.5 using 0.1 M KOH or 0.1 M HNO_3 solutions. After equilibration, the pH values were measured once again (pH_f), and the value of pH_{PZC} (point of zero charge) was determined from the plot of $\Delta pH = f(pH_0)$ ($\Delta pH = pH_0 - pH_f$). pH_{PZC} is the pH_0 value when $\Delta pH = 0$. From the graph in Figure 3, it is found that $\Delta pH = 0$ when the pH_0 value is 5.99. This means that the pH_{PZC} value of the halloysite material is also 5.99.

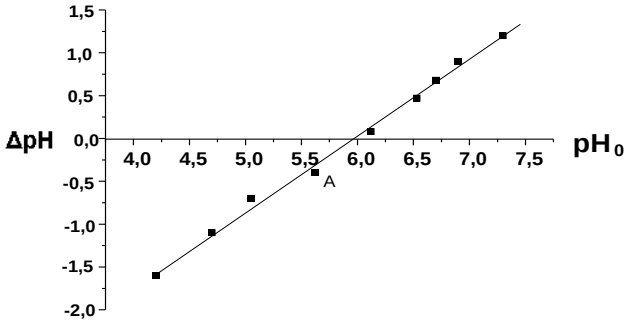

Figure 3. Variation of ΔpH versus pH_0.

2.4. Adsorption experiments

The adsorption experiments were carried out by mixing a dose of HAL with 50 mL of Ni^{2+} ion solution. HAL that absorbed Ni^{2+} ions was abbreviated as Ni-HAL. The parameters affecting the adsorption process were investigated including contact time varying from 10 to 120 min, initial pH of the solution ranging from 2.3 to 6.9, HAL mass ranging from 0.3 to 1.0 g. The experiments were performed at room temperature with continuous stirring at a speed of 400 rpm. After filtration to remove the solid, the remaining Ni^{2+} concentration was determined using the ICP-MS method (Thermo Scientific ICAP Q ICP-MS (Germany) at Hanoi University of Mining and Geology).

Adsorption capacity and efficiency are calculated by Equations (2.1) and (2.2), respectively [30]:

$$Q = (C_o - C).V/m \quad (2.1)$$

$$H = (C_o - C).100/C_o \quad (2.2)$$

where Q is the amount of metal ions adsorbed on the adsorbent at equilibrium (mg/g), C_o and C are the initial and equilibrium concentrations (mg/L) of Ni^{2+} ion in solution, respectively, V is the volume of solution (L), and m is the mass of adsorbent (g).

The experimental data obtained are analyzed using the Langmuir and Freundlich isotherm models [30]:

Langmuir linear equation:

$$\frac{C_e}{Q} = \frac{C_e}{Q_m} + \frac{1}{K_L.Q_m} \quad (2.3)$$

Freundlich linear equation:

$$LnQ = LnK_F + \frac{1}{n} LnC_e \quad (2.4)$$

where C_e (mg/L) is the equilibrium concentration of Ni^{2+}, Q (mg/g) is the adsorption capacity at equilibrium, Q_m (mg/g) is the maximum adsorption capacity, K_L (L/mg) is the Langmuir coefficient related to the adsorption energy, K_F (mg/g) and n are the constants of the Freundlich equation.

The adsorption kinetics is described by the pseudo-first-order and pseudo-second-order kinetic models using Equations (2.5) and (2.6), respectively [30].

$$Ln(Q_e - Q_t) = LnQ_e - k_1 t \quad (2.5)$$

$$t/Q_t = t/Q_e + 1/(k_2 . Q^2_e) \quad (2.6)$$

where Q_e is the adsorption capacity at equilibrium (mg/g), Q_t is the adsorption capacity at time t (mg/g), k_1 and k_2 are pseudo-first-order (min^{-1}) and pseudo-second-order (g/mg/min) rate constants, respectively.

2.5. Electrochemical experiments for desorption and recovery of nickel

2.5.1. Cyclic voltammetry scan of Ni^{2+} ion in reline DES

The cyclic voltammetry experiments were carried out using a three-electrode system connected to an Autolab PGSTAT20 (Metrohm) potentiostat. The working electrode (WE) was Au electrode (geometric area = 0.0201 cm^2), reference electrode (RE) was Ag, AgCl|Cl^- and the counter electrode (CE) was a platinum grid of a large area. The experiments were conducted on samples with a volume of 5 mL of reline solvent containing 0.005 M $Ni(NO_3)_2$ solution, using a scan potential range from -0.1 to -0.9 V and a scan rate of 50 $mV.s^{-1}$ at 60 ^oC.

The working electrode was polished with an alumina-water slurry on a smooth polishing cloth, then sonicated twice for 3 minutes and rinsed with Milli-Q water to remove any traces of alumina, and finally dried under nitrogen. The platinum counter electrode was cleaned by flaming to red glow. Before each experiment, the DES medium was purged with nitrogen for at least 20 minutes and kept under nitrogen atmosphere during all measurements.

2.5.2. Desorption of Ni^{2+} and deposition of Ni metal on the surface of Au plate electrode

The desorption of Ni^{2+} out of Ni-HAL and deposition of Ni metal were carried out in a three-electrode electrochemical cell: the WE was gold plate (geometric area = 1 cm^2), the RE was Ag, AgCl|Cl^- and the CE was a platinum grid of a large area. Nickel was deposited on the surface of Au plate into reline DES by applying current at 1, 2, 3, 5, and 7.5 mA; electrolytic time was studied from 1 to 5 hours with deposition potential $\leq$ – 0.6 V, T = 60 ^oC. After electrolysis, the desorbed HAL powder was filtered out of the mixture, then cleaned, dried, and the remaning Ni content in the powder was determined using the ICP-MS method.

3. RESULTS AND DISCUSSION

3.1. Effects of experimental factors on Ni^{2+} ion adsorption by HAL powder

3.1.1. Effect of contact time

The influence of contact time on the Ni^{2+} adsorption efficiency and capacity of HAL was investigated in the range of 10 ÷ 120 minutes. The results are displayed in Figure 4, showing that as the contact time increases, the adsorption capacity and efficiency increase. During the survey

period from 10 to 120 minutes, the adsorption efficiency and capacity increase rapidly in the first 40 minutes, then gradually increase and are almost stable from 80 minutes onwards. The adsorption efficiency and capacity increase gradually over time and reach stable values after 80 minutes, approximately 73 % and 3.6 mg/g, respectively. Thus, after 80 minutes, the Ni^{2+} adsorption process of HAL reaches equilibrium. To simultaneously achieve high adsorption efficiency and high adsorption capacity, a time of 80 minutes is chosen for further study.

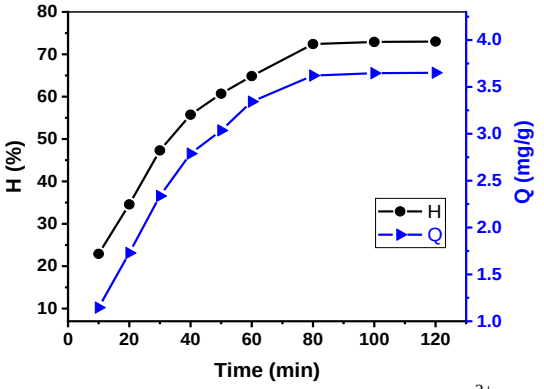

Figure 4. Effect of contact time on Ni^{2+} adsorption capacity and efficiency by HAL at initial concentration of 50 mg/L; mass of 0.5 g; pH 5.9.

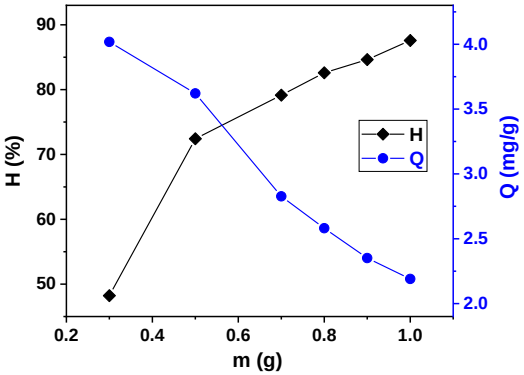

Figure 5. Effect of HAL mass on the adsorption capacity and efficiency of Ni^{2+} at initial concentration of 50 mg/L; pH 5.9; contact time of 80 minutes.

3.1.2. Effect of solution pH

Solution pH changes the surface properties of the adsorbent and existing forms of metal ion in solution [31], thus greatly affecting the removal of Ni^{2+} ions. The effect of pH was investigated under pH conditions varying around pH_{PZC} (5.99). However, the investigated pH range was less than or equal to 7 so that the main adsorbed species was $Ni^{2+}$and the formation of hydroxide precipitate of Ni^{2+} was avoided (Figure 6a).

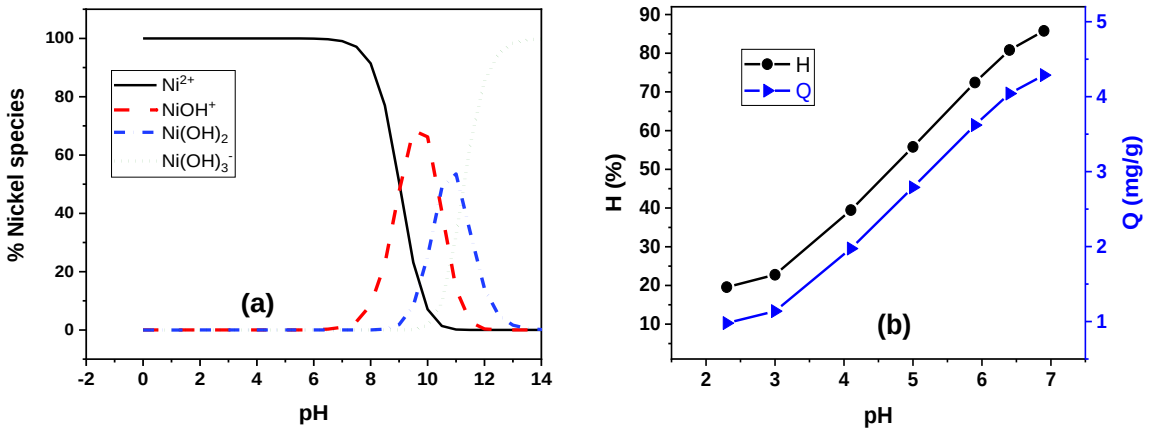

Figure 6. Variations of nickel species (a) and Ni^{2+} adsorption capacity and efficiency (b) according to pH at initial concentration of 50 mg/L; mass of 0.5 g; contact time of 80 minutes.

The results of the variation of adsorption efficiency and capacity according to pH are shown in Figure 6b. In the investigated pH range, the adsorption efficiency and capacity increase

as the pH increases. This result is explained by the fact that halloysite is protonated in acidic environment, then the particle surface will be positively charged, leading to a decrease in the number of HAL's adsorption centers and competitive adsorption between H^+ ions and Ni^{2+} ions, thus reducing the adsorption ability [32]. When the pH increases, the positive charge density of the surface decreases gradually, the adsorption ability of Ni^{2+} will gradually increase until the pH > pH_{PZC} will be favorable for the adsorption of Ni^{2+}. However, at pH 5.9 (initial pH) close to pH_{PZC}, the Ni^{2+} adsorption capacity is relatively favourable for treatment without pH adjustment, so natural pH 5.9 is chosen for the Ni^{2+} adsorption process in subsequent investigations.

3.1.3. Effect of material mass

The adsorption process was carried out with the mass of HAL varying from 0.3 g to 1.0 g. The results are shown in Figure 5. When the mass of HAL rises from 0.3 g to 0.5 g, the adsorption efficiency increases rapidly from 48.22 to 72.42 %, while the adsorption capacity decreases from 4.02 down to 3.62 mg/g. The adsorption efficiency increases significantly with the increase of adsorption sites due to the adsorbent mass increases [10]. The adsorption efficiency then increases slowly as the amount of adsorbent continues to increase up to 1.0 g. However, if the amount of adsorbent continues to increase, the efficiency is almost unchanged because the adsorption process reaches equilibrium, meanwhile the adsorption capacity decreases gradually. To achieve high adsorption efficiency (82.59 %), a mass of HAL of 0.8 g is chosen for studying the adsorption of Ni^{2+} ions. This result shows that the adsorption ability of HAL is quite high for Ni^{2+}, with the adsorption efficiency is close to As(III) (82.4 %) [9], but smaller than Pb^{2+} (90.75 %) [13].

3.2. Characterization of HAL before and after adsorption process

The characterizations of HAL powder before and after adsorption process are analyzed using FT-IR and SEM-EDX. The FT-IR spectra shows that Ni^{2+} adsorption process does not change the functional groups in HAL molecule (Figure 7). The SEM image of HAL and Ni-HAL is shown in Figure 8. The surface morphology of HAL and Ni-HAL is nanotube-like. After the Ni^{2+}adsorption process, there is no significant change in particle size and shape. The EDX spectra confirms the presence of nickel in HAL after adsorption process, however the amount of Ni is very little (Figure 8).

3.3. Adsorption isotherm

The adsorption of Ni^{2+} was carried out under the studied appropriate conditions: 0.8 g of HAL in 50 mL of Ni^{2+} solution, contact time of 80 minutes at natural pH 5.9, and room temperature (25 ^oC) with varying the initial Ni^{2+} concentration from 10 to 80 mg/L. The remaining Ni^{2+} concentration at equilibrium (C_e) can be determined, from which the values of lnC_e, lnQ, and ratio of C_e/Q can be calculated to construct the Langmuir (Figure 9a) and Freundlich (Figure 9b) isothermal plots. Based on them the experimental Langmuir parameters such as the maximum adsorption capacity (Q_m) and the Langmuir constant (K_L) as well as the experimental Freundlich constants (K_F, n) are calculated (Table 1). The results show that the adsorption of Ni^{2+} on HAL follows the Langmuir isotherm adsorption model, which is consistent with many published results using HAL material for adsorption of heavy metals and organic pigments [11].

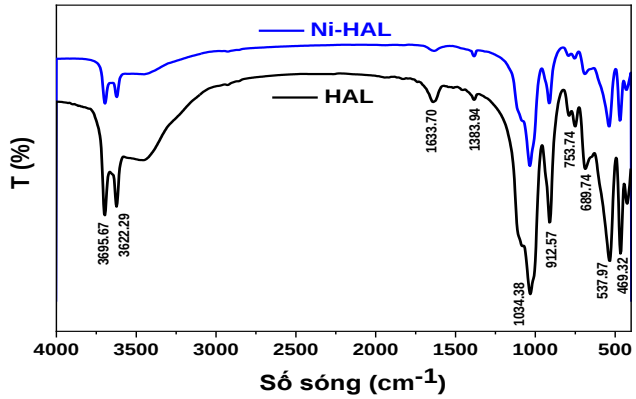

Figure 7. FT-IR spectra of HAL before and after Ni^{2+} adsorption process.

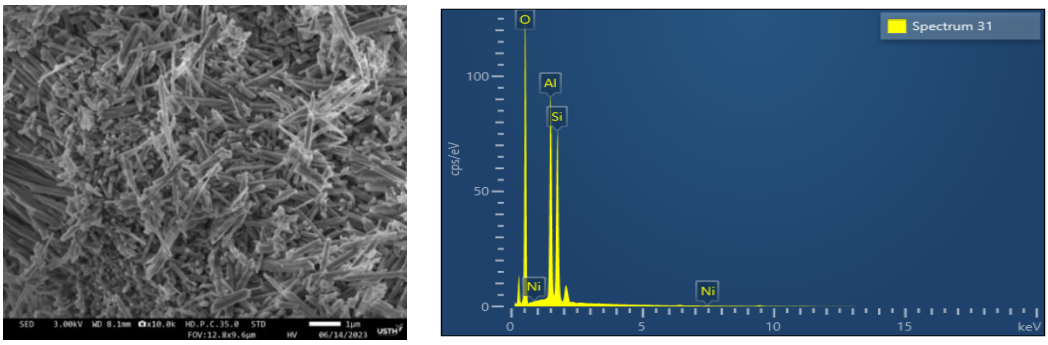

Figure 8. SEM-EDX images of HAL after Ni^{2+} adsorption process.

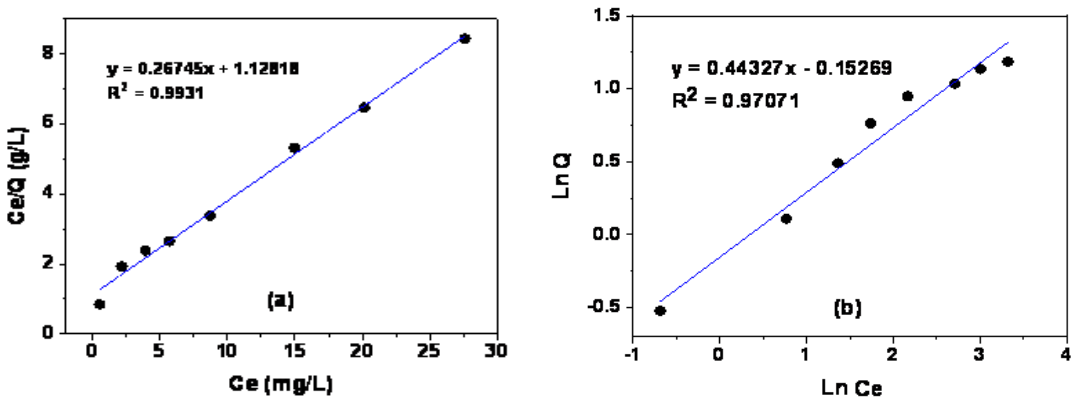

Figure 9. Langmuir (a) and Freundlich (b) isotherm plots for the adsorption of Ni^{2+} onto HAL.

Table 1. Adsorption isotherm parameters.

Langmuir			**Freundlich**		
Q_m (mg/g)	K_L (L/mg)	R^2	n	K_F (mg/g)	R^2
3.739	0.2370	0.9931	2.2560	0.8585	0.9707

3.4. Adsorption kinetics

Based on the study results of the effect of adsorption time on the Ni^{2+} adsorption ability of HAL under the following conditions: initial Ni^{2+} concentration of 50 mg/L, HAL mass of 0.8 g, at pH = 5.9 and at room temperature of 25 ^{o}C, the kinetic equations of pseudo-first-order (Equation 2.5) and pseudo-second-order (Equation 2.6) are built, and the results are shown in Figure 10.

From Figure 10, the adsorption rate constants (k) and adsorption capacity at equilibrium (Q_e) can be calculated (Table 2). The Q_e value calculated according to the pseudo-first order kinetic equation (9.813 mg/g) is far different from the experimentally determined Q_e value (3.651 mg/g), meanwhile the Q_e value calculated by the pseudo-second order kinetic equation (4.724 mg/g) is closer to the experimentally determined Q_e value. In addition, the regression coefficient of the pseudo-second order kinetic equation reaches $R^2 = 0.9911 \approx 1$, while the regression coefficient of the pseudo-first order kinetic equation (0.9269) is far from 1. This result proves that the adsorption process of Ni^{2+} by HAL follows the pseudo-second order kinetic equation. The determined adsorption rate constant is 0.0071 g/mg/min.

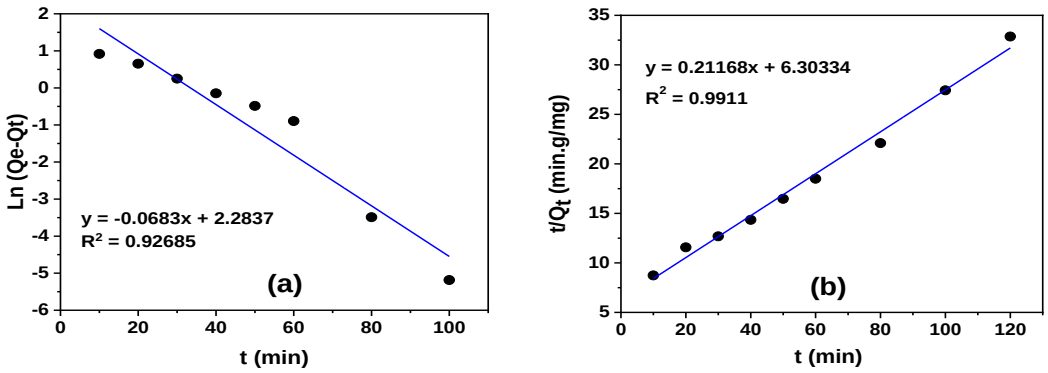

Figure 10. Description of the experimental data according to pseudo-first-order kinetic equation (a) and pseudo-second-order kinetic equation (b) for adsorption of Ni^{2+} onto HAL.

Table 2. Adsorption kinetic parameters.

pseudo-first-order kinetic equation			**pseudo-second-order kinetic equation**			**Q_e experiment (mg/g)**
Q_e (mg/g)	**k_1 (min^{-1})**	**R^2**	**Q_e (mg/g)**	**k_2 (g/mg/min)**	**R^2**	
9.813	0.0683	0.9269	4.724	0.0071	0.9911	3.651

3.5. Desorption of Ni^{2+} from Ni-HAL and recovery of Ni metal by electrocdeposition method

The electrochemical properties of Ni^{2+} in reline solvent are shown in Figure 11. From this, it can be seen that the deposition of Ni metal on the surface of Au electrode can be caried out at potentials ≤ -0.58 V. Thus, Ni^{2+} ions are desorbed from Ni-HAL and then Ni metal is recovered by electrodeposition method in reline solvent using current application techniques. The mechanism of Ni deposition on the Au electrode and its dissolution from the Au electrode can be described as follows:

Step 1: The complex between Ni^{2+} of Ni-HAL with Cl^- of reline was formed ($NiCl_n^{2-n}$)., Then, the reduction of Ni^{2+} (of $NiCl_n^{2-n}$) to Ni metal on the electrode surface occurred:

$$NiCl_n^{2-n} + 2e^- \rightarrow Ni + nCl^- \quad (3.1)$$

Step 2: Ni metal was stripped to Ni^{2+}:

$$Ni - 2e^- \rightarrow Ni^{2+} \quad (3.2)$$

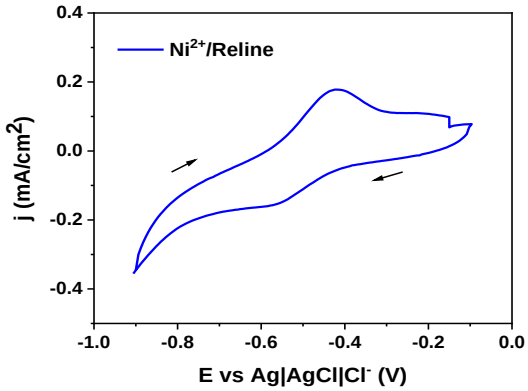

Figure 11. Cyclic voltammogram of 0.005 M Ni^{2+} in the reline, scan rate of 50 $mV.s^{-1}$, temperature of 60 ^oC.

The deposition of Ni on the surface of Au plate electrode is expressed in Figures 12 and 13.

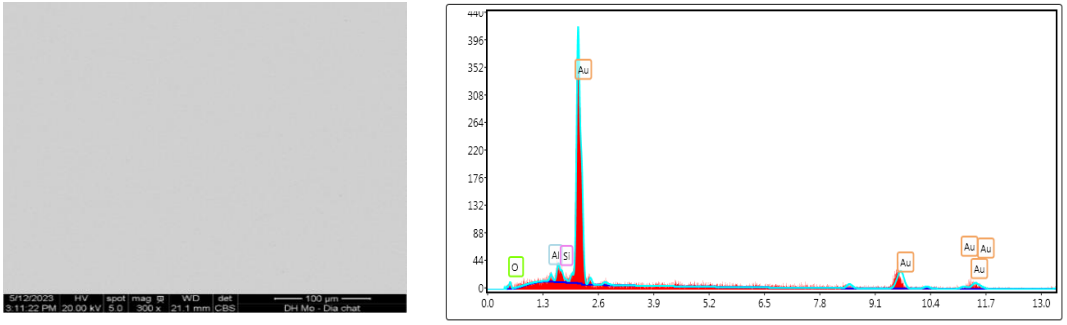

Figure 12. SEM-EDX image of the surface of Au plate electrode before electrolysis of Ni-HAL.

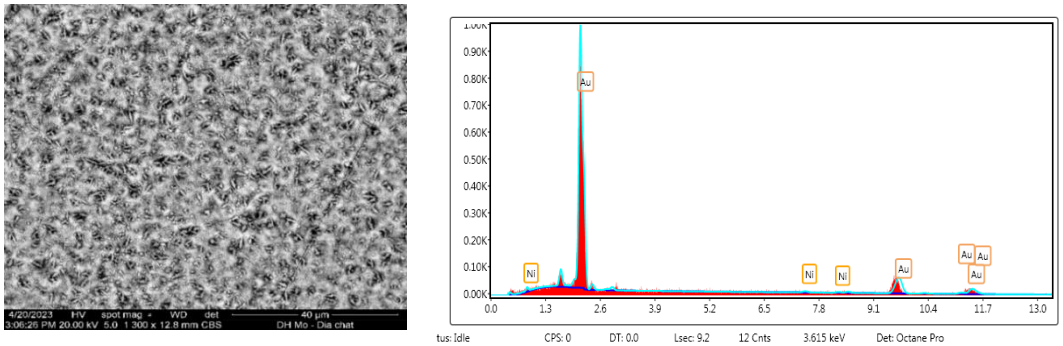

Figure 13. SEM-EDX image of the surface of Au plate electrode after electrolysis of Ni-HAL.

Figure 12 shows the smooth surface of the Au plate electrode before electrolysis. The EDX results indicate three picks for Au, Al, and Si elements appearing on the surface of Au plate electrode (Figure 12). However, after electrolysis, Ni metal evenly covered the Au plate electrode due to EDX analysis (Figure 13).

The cathodic polarization of the Au electrode at different applied current values was conducted with different electrolytic times at a temperature of 60 °C. The recovery efficiency of Ni is shown in Table 3.

Table 3. Recovery efficiency of Ni (H %) from 0.5 g of Ni-HAL at different applied currents and electrolytic times.

H %					
I (mA) / t (hour)	**1.0**	**2.0**	**3.0**	**5.0**	**7.5**
1	56.39	58.26	60.32	62.25	65.81
2	64.23	67.83	68.44	71.34	73.76
3	71.11	73.88	75.48	78.47	80.52
4	76.68	79.23	82.14	84.95	87.24
5	81.62	85.29	88.05	90.18	92.65

It was found that Ni^{2+}ions are desorbed from the HAL material and Ni metal is deposited on the surface of Au plate electrode. Table 3 shows the variation of the recovery efficiency of Ni according to applied current and electrolytic time. The applied current increases leading to an increase in the deposited amount of Ni on the surface of Au electrode, therefore the recovery efficiency of Ni increases. The electrolytic time rises leading to a rise in the deposited amount of Ni on the surface of Au electrode, thus the recovery efficiency of Ni increases, reaching 92.65 % after 5 hours of electrolysis at an applied current of 7.5 mA. After electrolysis, the HAL material is not dissolved in the reline solvent, thereby it is hoped that it can be reused after the desorption process.

4. CONCLUSIONS

HAL clay was used to study the adsorption/desorption of Ni^{2+}ions from aqueous solution. The obtained results indicated that the adsorption process was influenced by factors such as pH, mass of adsorbent, and contact time. Ni^{2+} adsorption efficiency and capacity reached 82.59 % and 2.58 mg/g, respectively, under appropriate conditions. The results of adsorption isotherms showed that the adsorption of Ni^{2+} ions using HAL powder followed the Langmuir isothermal model with a maximum monolayer adsorption capacity of 3.739 mg/g. The experimental data of adsorption kinetics confirmed that the Ni^{2+} adsorption process followed the pseudo-second-order law with a correlation coefficient (R^2) of 0.9911. The recovery efficiency of nickel reached 92.65 % from the adsorbed HAL material by electrodeposition on the surface of Au plate electrode at an applied current of 7.5mA after 5 hours in an electrolytic solution of reline. In the electrolyte of reline, HAL was not dissolved and can be reused after desorption.

Acknowledgements. The authors would like to sincerely thank the financial support of the project from the Ministry of Education and Training (code: B2022-MDA-03) for completing this work.

CRediT authorship contribution statement. Le Thi Duyen: Idea, Methodology, Supervision, Writing original draft, Editing; Le Thi Phuong Thao: Writing review, Investigation; Cong Tien Dung: Formal analysis, Editing; Nguyen Viet Hung, Ha Manh Hung, Mai Van Tien: Investigation; Nguyen Thi Thanh Thao, Bui Hoang Bac: Preparation of materials.

Declaration of competing interest. The authors declare that they have no known competing financial interests or personal relationships that could have appeared to influence the work reported in this paper.

REFFERENCES

1. Sharma R., Saini K. C., Rajput S., Kumar M., Mehariya S., Karthikeyan O. P., Bast F.- Environmental Friendly Technologies for Remediation of Toxic Heavy Metals: Pragmatic Approaches for Environmental Management*;* Aravind, J., Kamaraj, M., Karthikeyan, S., Eds.; Springer International Publishing: Cham (2022) 199-223.
2. Jadoun S., Fuentes J. P., Urbano B. F., Yáñez J. - A review on adsorption of heavy metals from wastewater using conducting polymer-based materials, Journal of Environmental Chemical Engineering **11** (2023) 109226.
3. Vakili M., Rafatullah M., Yuan J., Zwain H. M., Mojiri A., Gholami Z., Gholami F., Wang W., Giwa A. S., Yu Y., Cagnetta G., Yu G. - Nickel ion removal from aqueous solutions through the adsorption process: a review **37** (2021) 755-778.
4. Noman E., Al-Gheethi A., Saphira Radin Mohamed R. M., Al-Sahari M., Hossain M. S., Vo D.-V. N., Naushad M. - Sustainable approaches for nickel removal from wastewater using bacterial biomass and nanocomposite adsorbents: A review, Chemosphere **291** (2022) 132862.
5. Program N. T. - National Toxicology Program, Report on Carcinogens, 2016.
6. Toufik C., Atmane B. - Impact of Influencing Parameters on the Adsorption of Nickel by Kaolin in an Aqueous Medium, Analytical and Bioanalytical Chemistry Research **9** (2022) 381-399.
7. Yuan P., Tan D., Annabi-Bergaya F. - Properties and applications of halloysite nanotubes: recent research advances and future prospects, Applied Clay Science **112-113** (2015) 75-93.
8. Zhang Y., Tang A., Yang H., Ouyang J. - Applications and interfaces of halloysite nanocomposites, Applied Clay Science **119** (2016) 8-17.
9. Aljohani N. S., Kavil Y. N., Al-Farawati R. K., Saad Alelyani S., I Orif M., Shaban Y. A., Al-Mhyawi S. R., Aljuhani E. H., Abdel Salam M. - The effective adsorption of arsenic from polluted water using modified Halloysite nanoclay, Arabian Journal of Chemistry **16** (2023) 104652.
10. Abdel-Fadeel M. A., Aljohani N. S., Al-Mhyawi S. R., Halawani R. F., Aljuhani E. H., Salam M. A. - A simple method for removal of toxic dyes such as Brilliant Green and Acid Red from the aquatic environment using Halloysite nanoclay, Journal of Saudi Chemical Society **26** (2022) 101475.
11. Anastopoulos I., Mittal A., Usman M., Mittal J., Yu G., Núñez-Delgado A., Kornaros M. - A review on halloysite-based adsorbents to remove pollutants in water and wastewater, J. Mol. Liq. **269** (2018) 855-868.

12. Altun T., Ecevit H. - Adsorption of malachite green and methyl violet 2B by halloysite nanotube: Batch adsorption experiments and Box-Behnken experimental design, Mater. Chem. Phys. **291** (2022) 126612.
13. Bac B. H., Nguyen H., Thao N. T. T., Duyen L. T., Hanh V. T., Dung N. T., Khang L. Q., An D. M. - Performance evaluation of nanotubular halloysites from weathered pegmatites in removing heavy metals from water through novel artificial intelligence-based models and human-based optimization algorithm, Chemosphere **282** (2021) 131012.
14. Chen J. H., Wang Y. J., Zhou D. M., Cui Y. X., Wang S. Q., Chen Y. C. - Adsorption and desorption of Cu(II), Zn(II), Pb(II), and Cd(II) on the soils amended with nanoscale hydroxyapatite, Environmental Progress & Sustainable Energy **29** (2010) 233-241.
15. Feng Y., Gong J. L., Zeng G. M., Niu Q. Y., Zhang H. Y., Niu C. G., Deng J. H., Yan M. - Adsorption of Cd (II) and Zn (II) from aqueous solutions using magnetic hydroxyapatite nanoparticles as adsorbents, Chem. Eng. J. **162** (2010) 487-494.
16. Xia X., Shen J., Cao F., Wang C., Tang M., Zhang Q., Wei S. - A facile synthesis of hydroxyapatite for effective removal strontium ion, J. Hazard. Mater. **368** (2019) 326-335.
17. Aliabadi M., Irani M., Ismaeili J., Najafzadeh S. - Design and evaluation of chitosan/hydroxyapatite composite nanofiber membrane for the removal of heavy metal ions from aqueous solution, Journal of the Taiwan Institute of Chemical Engineers **45** (2014) 518-526.
18. Kede M. L. F. M., Mavropoulos E., da Rocha N. C. C., Costa A. M., da Silva M. H. P., Moreira J. C., Rossi A. M. - Polymeric sponges coated with hydroxyapatite for metal immobilization, Surf. Coat. Technol. **206** (2012) 2810-2816.
19. Peld M., Tõnsuaadu K., Bender V. - Sorption and Desorption of Cd2+ and Zn2+ Ions in Apatite-Aqueous Systems, Environ. Sci. Technol. **38** (2004) 5626-5631.
20. Thakur P., Moore R. C., Choppin G. R. - Sorption of U(VI) species on hydroxyapatite, Radiochimica Acta **93** (2005) 385-391.
21. Rehman S., Huang Z., Wu P., Ahmed Z., Ye Q., Liu J., Zhu N. - Adsorption of lead and antimony in the presence and absence of EDTA by a new vermiculite product with potential recyclability, Environmental Science and Pollution Research **28** (2021) 49112-49124.
22. Quaghebeur M., Rate A., Rengel Z., Hinz C. -Heavy Metals in the Environment Desorption Kinetics of Arsenate from Kaolinite as Influenced by pH. Journal of environmental quality, **34** (2005) 479-486.
23. Xie S., Wen Z., Zhan H., Jin M. -An Experimental Study on the Adsorption and Desorption of Cu(II) in Silty Clay. Geofluids, **2018** (2018) 3610921.
24. Li H., Sheng G., Teppen B., Johnston C., Boyd S. -Sorption and Desorption of Pesticides by Clay Minerals and Humic Acid-Clay Complexes. Soil Science Society of America Journal - SSSAJ, **67** (2003) 122-131.
25. Maziarz P., Matusik J., Radziszewska A. -Halloysite-zero-valent iron nanocomposites for removal of Pb(II)/Cd(II) and As(V)/Cr(VI): Competitive effects, regeneration possibilities and mechanisms. Journal of Environmental Chemical Engineering, **7** (2019) 103507.
26. Abbott A. P., Ballantyne A., Harris R. C., Juma J. A., Ryder K. S., Forrest G. -A Comparative Study of Nickel Electrodeposition Using Deep Eutectic Solvents and Aqueous Solutions. Electrochim. Acta, **176** (2015) 718-726.

27. Gong K., Hua Y.-x., Xu C.-y., Zhang Q.-b., Li Y., Ru J.-j., Jie Y.-f. -Electrodeposition behavior of bright nickel in air and water-stable betaine·HCl–ethylene glycol ionic liquid. Transactions of Nonferrous Metals Society of China, **25** (2015) 2458-2465.
28. You Y. H., Gu C. D., Wang X. L., Tu J. P. -Electrodeposition of Ni–Co alloys from a deep eutectic solvent. Surf. Coat. Technol., **206** (2012) 3632-3638.
29. Yang H. Y., Guo X. W., Chen X. B., Wang S. H., Wu G. H., Ding W. J., Birbilis N. -On the electrodeposition of nickel–zinc alloys from a eutectic-based ionic liquid. Electrochim. Acta, **63** (2012) 131-138.
30. Gupta N., Kushwaha A. K., Chattopadhyaya M. C. -Adsorption studies of cationic dyes onto Ashoka (Saraca asoca) leaf powder. Journal of the Taiwan Institute of Chemical Engineers, **43** (2012) 604-613.
31. Sheha R.R., Sorption behavior of Zn(II) ions on synthesized hydroxyapatites, J. Colloid Interface Sci., **310** (2007) 18-26.
32. Dou W., Deng Z., Fan J., Lin Q., Wu Y., Ma Y., Li Z. -Enhanced adsorption performance of La(III) and Y(III) on kaolinite by oxalic acid intercalation expansion method. Applied Clay Science, **229** (2022) 106693.